Supplementary Information:

Atomic sites and stability of Cs^+ captured within zeolitic nanocavities

Kaname Yoshida,* Kazuaki Toyoura, Katsuyuki Matsunaga, Atsushi Nakahira, Hiroki Kurata, Yumi H. Ikuhara, and Yukichi Sasaki

Contents

I. Elemental Analysis
Figure S1| Energy dispersive X-ray analysis.

II. Evaluation of Image Quality
Figure S2| Raw HAADF-STEM images and FFT patterns.
Figure S3| Raw AC-HRTEM images and FFT patterns.

III. Image Simulations
Figure S4: Simulated HAADF-STEM images of NaA projected along [001].
Figure S5: Simulated HAADF-STEM images of CsA projected along [001].
Figure S6: Simulated AC-HRTEM images of NaA projected along [001].
Figure S7: Simulated AC-HRTEM images of CsA projected along [001].

IV. *Ab initio* Molecular Dynamics
Figure S8| Framework structure models for AIMD calculation.

I. Elemental Analysis

Energy dispersive X-ray (EDX) spectra were measured from an area scanned using the electron beam (15 keV) of a field emission electron microscope (FE-SEM). For FE-SEM observations, powdered samples were dispersed on aluminum specimen mounts and coated with very thin amorphous carbon. Cation atomic ratios normalized according to the atomic ratio of silicon were estimated from each spectrum.

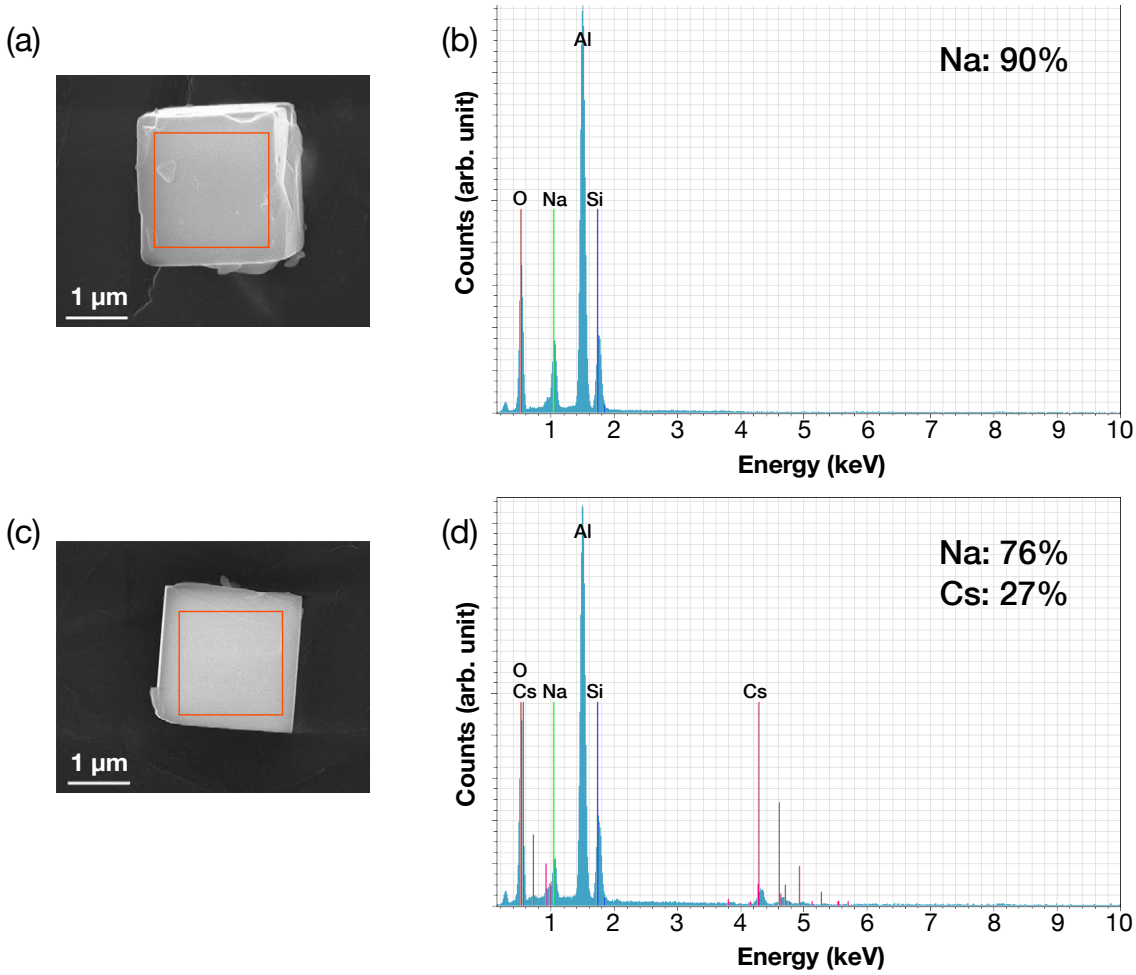

Figure S1: Energy dispersive X-ray (EDX) analysis. a,c, FE-SEM images of NaA and Cs^+-exchanged NaA, respectively. Orange rectangles in each image indicate the analysis area. **b,d,** EDX spectra of NaA and Cs^+-exchanged NaA, respectively. Cation atomic ratios normalized according to the atomic ratio of silicon are shown in each spectrum.

II. Evaluation of image quality

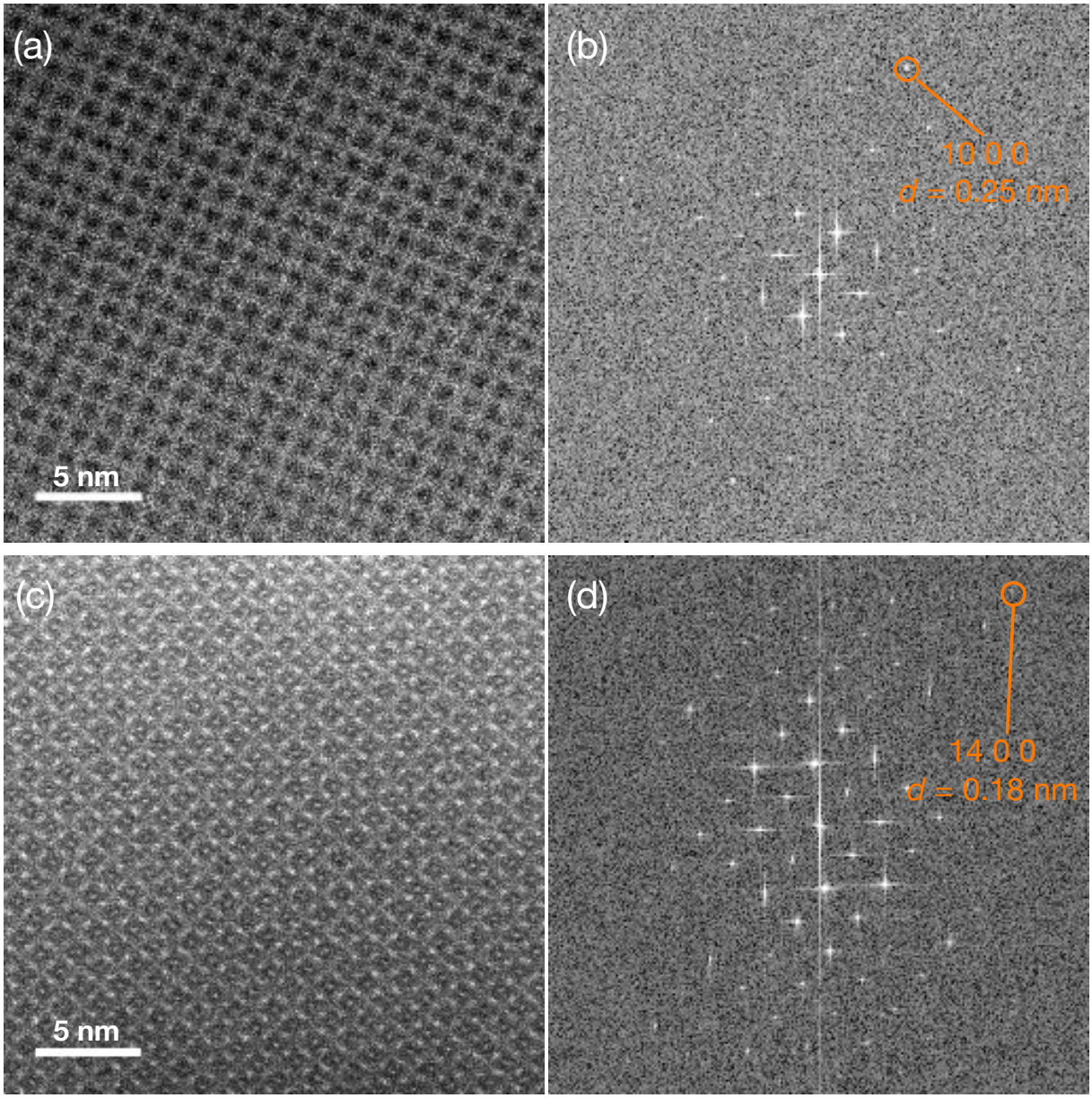

Figure S2: FFT Patterns of HAADF-STEM images. a,c, Raw HAADF-STEM images of NaA and Cs^+-exchanged NaA, respectively. **b,d,** FFT patterns of HAADF-STEM images of NaA and Cs^+-exchanged NaA, respectively.

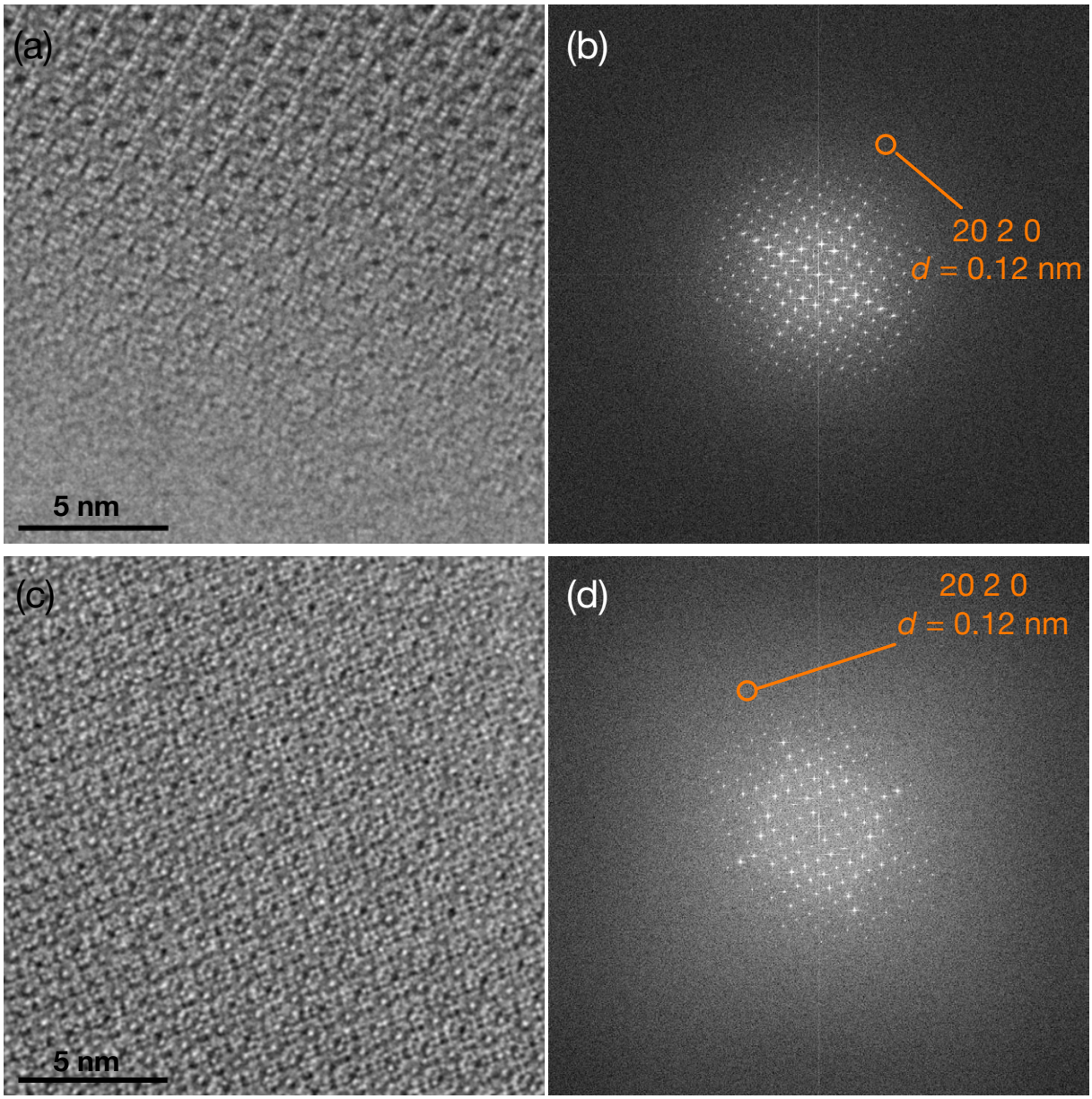

Figure S3: FFT Patterns of AC-HRTEM images. a,c, Raw AC-HRTEM images of NaA and Cs^+-exchanged NaA, respectively. **b,d,** FFT patterns of HAADF-STEM images of NaA and Cs^+-exchanged NaA, respectively.

III. Image Simulations

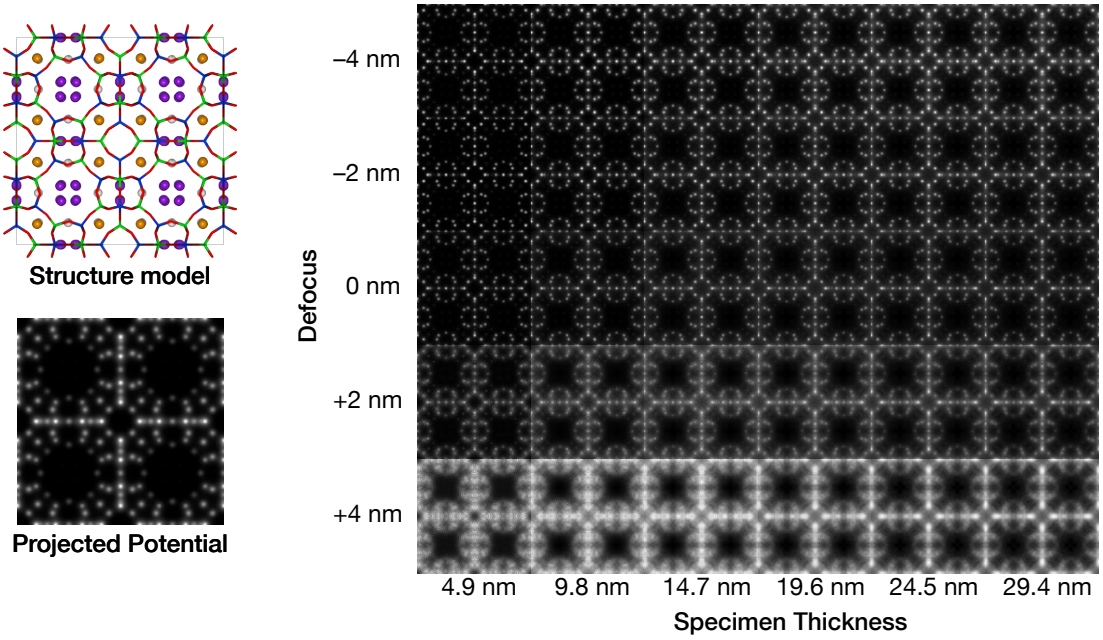

Figure S4: Simulated HAADF-STEM images of NaA projected along [001]. The parameters for the simulation were: 200 kV, C_3 = 0 mm convergence angle = 25 mrad, 73-194 mrad collection angle at defocus from –4 to + 4 nm and thickness from 4.9 to 29.4 nm.

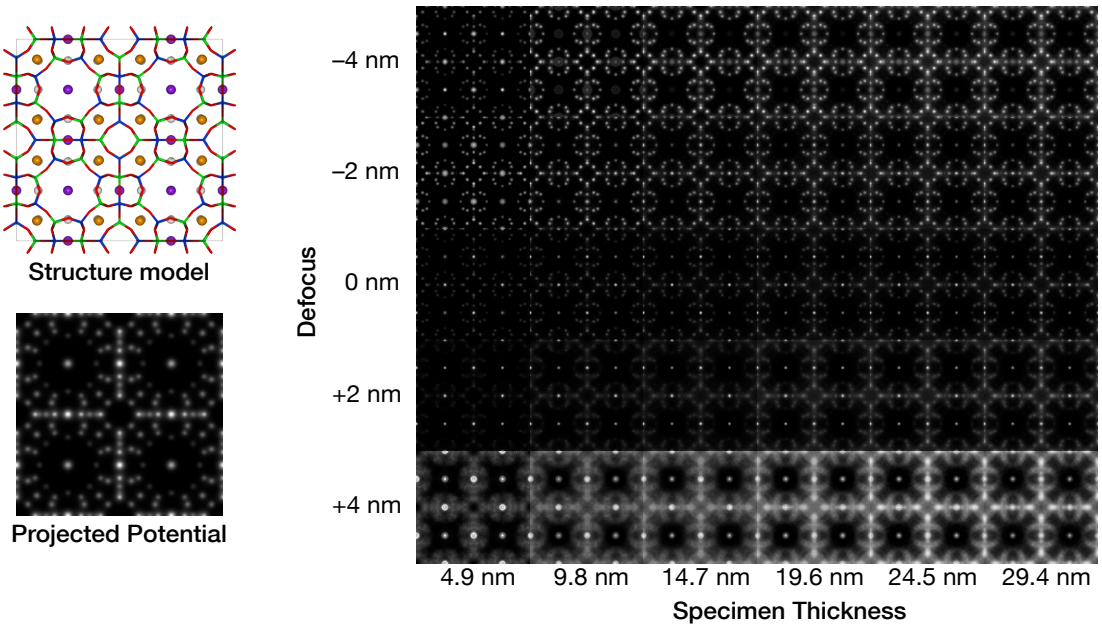

Figure S5: Simulated HAADF-STEM images of Cs-exchanged NaA projected along [001]. The parameters for the simulation were: 200 kV, C_3 = 0 mm convergence angle = 30 mrad, 73-194 mrad collection angle at defocus values from –4 to + 4 nm and thickness from 4.9 to 29.4 nm. In this model, Na atoms located at Na2 sites were replaced with Cs atoms. The positions of Cs atoms were modified to the center of S8R.

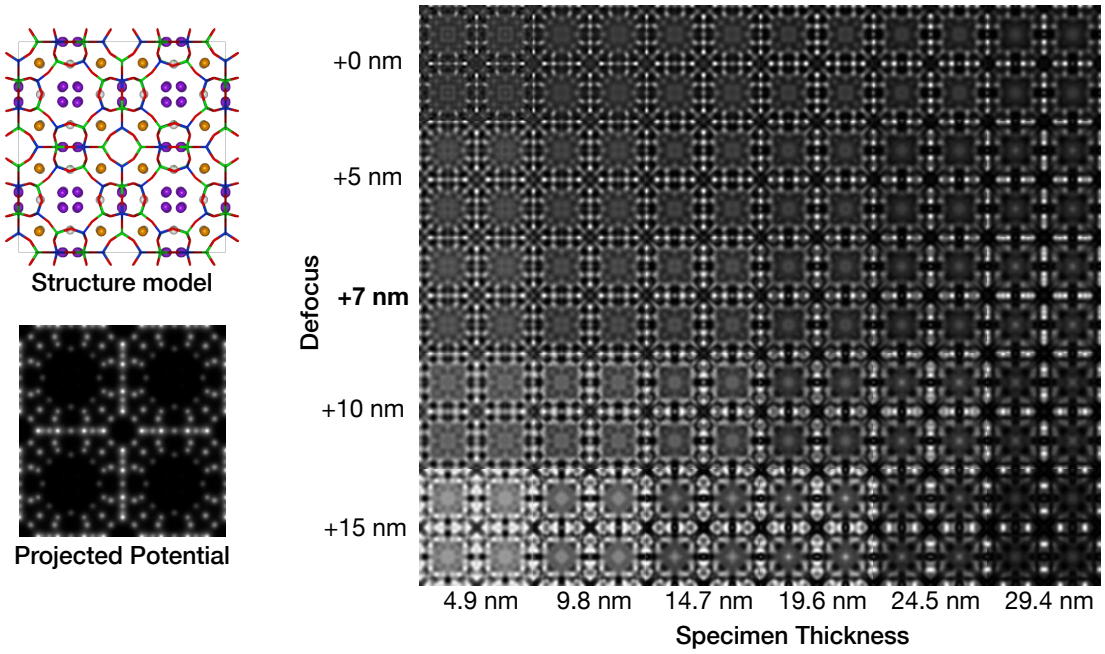

Figure S6: Simulated AC-HRTEM images of NaA projected along [001]. The parameters for the simulation were: 200 kV, C_3 = –15 µm convergence at defocus values from 0 to + 15 nm and thickness from 4.9 to 29.4 nm. The optimum defocus (= Scherzer defocus) is +7 nm.

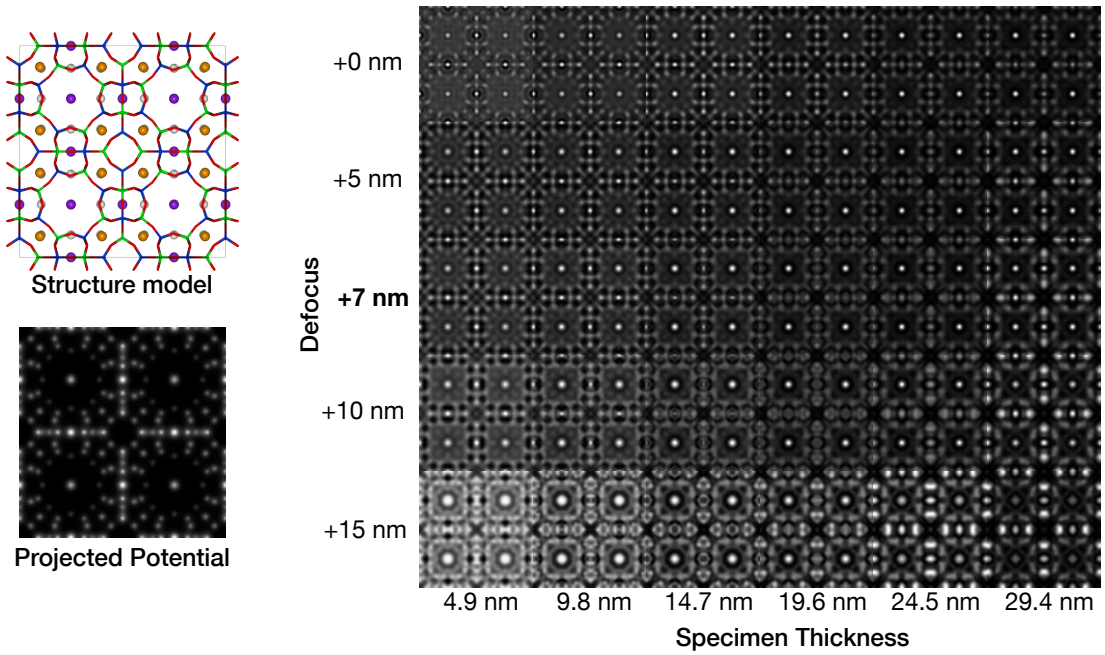

Figure S7: Simulated AC-HRTEM images of Cs-exchanged NaA projected along [001]. The parameters for the simulation were: 200 kV, C_3 = –15 µm convergence at defocus values from 0 to + 15 nm and thickness from 4.9 to 29.4 nm. The optimum defocus (= Scherzer defocus) is +7 nm.

IV. Ab initio molecular dynamics

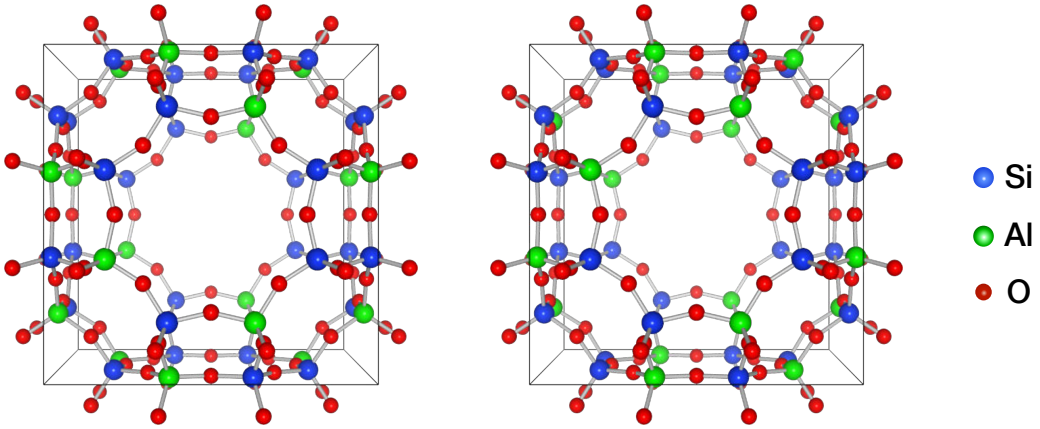

Figure S8: Framework Structure models for AIMD calculation. According to Löwenstein's law, two structure models with different aluminum sites permitted the $Na_9Al_9Si_{15}O_{48}$ cubic (a = 1.23 nm) unit. For AIMD simulations, the type-A framework was selected because of the slightly lower calculated energy by 0.05 eV, which can be qualitatively explained by Dempsey's law.